1962

The thallium-indium phase diagram as a function of composition, temperature, and pressure

Robert Wagner Meyerhoff
Iowa State University

THE THALLIUM-INDIUM PHASE DIAGRAM AS A FUNCTION OF COMPOSITION, TEMPERATURE, AND PRESSURE

by

Robert Wagner Meyerhoff

A Dissertation Submitted to the
Graduate Faculty in Partial Fulfillment of
The Requirements for the Degree of
DOCTOR OF PHILOSOPHY

Major Subject: Physical Chemistry

Approved:

Signature was redacted for privacy.

In Charge of Major Work

Signature was redacted for privacy.

Head of Major Department

Signature was redacted for privacy.

Dean of Graduate College

Iowa State University
of Science and Technology
Ames, Iowa

1962

TABLE OF CONTENTS

	Page
INTRODUCTION	1
EXPERIMENTAL PROCEDURE	7
Sample Preparation	7
X-ray Measurements	9
Determination of Electrical Resistivity	10
RESULTS	16
X-ray Measurements	16
The Thallium-Indium Phase Diagram at Ambient Pressure	24
The Effect of Pressure on the Thallium-Indium Phase Diagram	30
DISCUSSION	36
SUMMARY	41
LITERATURE CITED	42
ACKNOWLEDGMENTS	44
APPENDIX	45

INTRODUCTION

While a large amount of work has been undertaken to determine the effect of pressure on most of the equilibria possible in one and two component systems, virtually no work has been carried out in the study of the effect of both pressure and temperature on solid-solid equilibria in binary metallic systems. Bridgman (1-6) has done the majority of the limited work on such solid-solid equilibria. Bridgman's work is summarized in a series of six articles published from 1953 to 1957. However, all of his work was at room temperature.

The cardinal objective of this investigation was the determination of the thallium-indium phase diagram as a function of composition, temperature, and pressure. The majority of the work to be described was concentrated on the thallium-rich end of the phase diagram. Some reasons for this choice are the following. First, the thallium-rich region of the phase diagram shown in Figure 1 is based on a small amount of data reported by Guttman (7) and Valentiner (8), thus additional study of this region would be profitable. Second, no work had been done to determine the

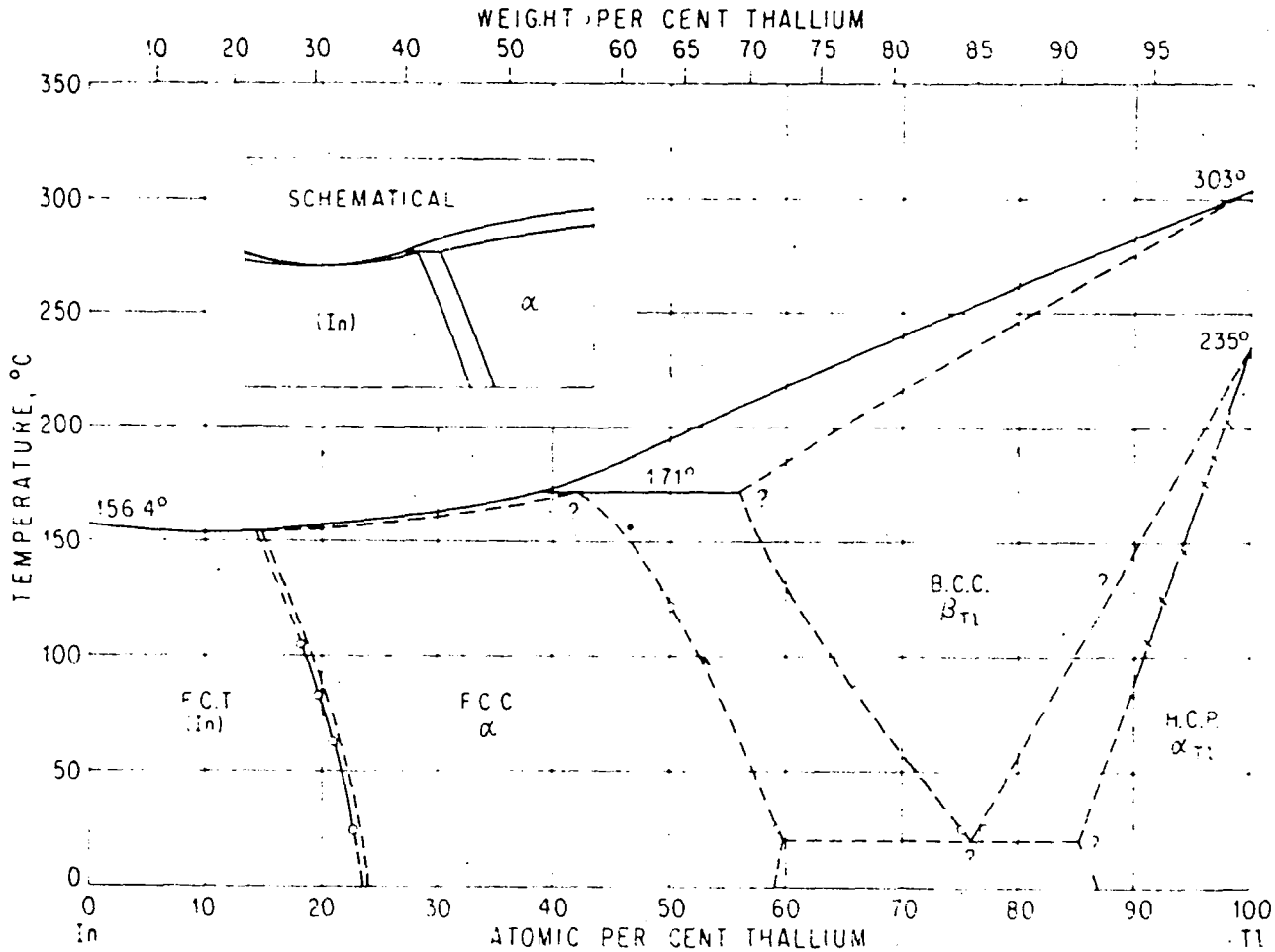

Figure 1. The thallium-indium phase diagram as given by Hansen (14)

effect of pressure on the HCP-BCC transformation of thallium when indium is present in solid solution; however, the effect of pressure on this transformation in pure thallium had been determined by both Werner (9) and Bridgman (10). Third, Bridgman (3,10) has reported the existence of an additional phase of pure thallium which is stable at high pressures. This has been corroborated by Kennedy and LaMori (11) and Boyd and England (12). The temperature-pressure phase diagram of pure thallium reported by Bridgman (10) is shown in Figure 2. The effect of indium on the transformation of HCP-thallium to the high pressure form at room temperature has been investigated by Bridgman (3). The results of his investigation indicated that at room temperature the pressure necessary for the stability of the high pressure form decreases with the addition of indium and approaches ambient pressure in the region of 30 to 40 per cent indium. Bridgman's results are consistent with an earlier phase diagram of the thallium-indium system (13); however, Bridgman's results are inconsistent with the more recent phase diagram (14) shown in Figure 1 which indicates a maximum solubility of about 15 atomic per cent indium in HCP-thallium. Fourth, Schneider and Heymer (15) and Sekito (16)

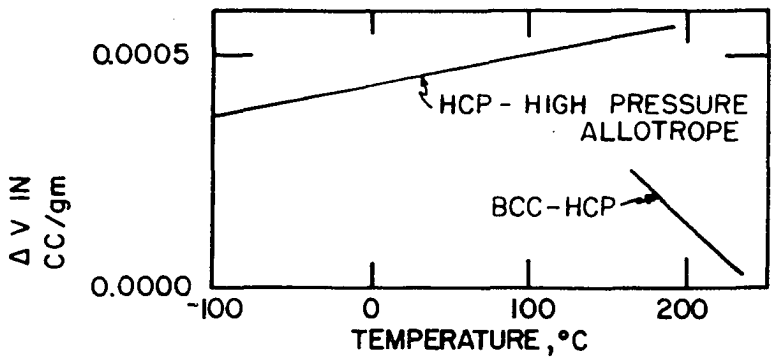

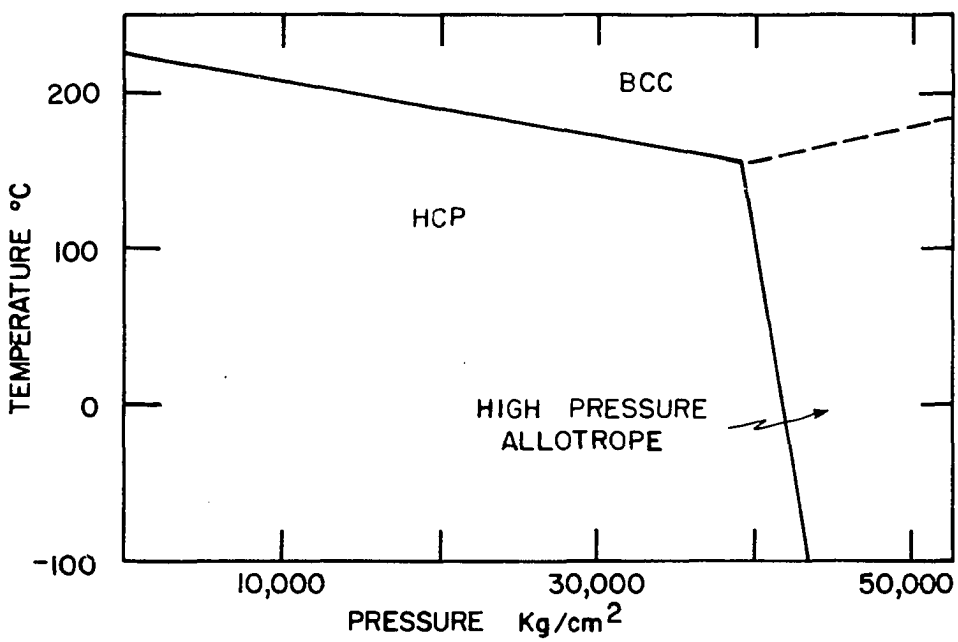

Figure 2. Bridgman's (10) results for the allotropic transformations of thallium

have reported finding a face centered cubic (FCC) allotrope of thallium at ambient pressure. These observations of a metastable FCC allotrope of thallium at ambient pressure coupled with the results of Bridgman (3) suggest that the structure of the high pressure allotrope of thallium may be FCC. One of the prime objectives of the present investigation was to determine whether the pressure-composition-temperature diagram of the thallium-indium system is consistent with this hypothesis.

The determination of electrical resistivity as a function of pressure and temperature was the primary method used in this investigation to determine the positions of the various phase boundaries. Thermal analyses were unsatisfactory for the determination of the phase diagram at ambient pressure because of the small enthalpy changes associated with the transformations. For instance, the enthalpy change associated with the HCP-BCC transformation in pure thallium is only about 0.4 calories per gram while, in contrast, the change in electrical resistivity is several per cent. Similarly, pressure-volume measurements were undesirable because of the small volume change associated with the HCP-BCC transformation; this volume change was found by Bridgman

(3) to be of the order of 0.1 per cent. With addition of indium to thallium, this small volume change would be smeared over a range of pressure and temperature and would become undetectable by conventional pressure-volume measurements. Thus only x-ray measurements were made to supplement the resistivity data. The x-ray measurements were made at room temperature and ambient pressure to determine ΔV of mixing for the system and to determine the effect of indium on the lattice constants of HCP-thallium.

EXPERIMENTAL PROCEDURE

Sample Preparation

The majority of the alloys were prepared from thallium and indium having a purity of 99.999 per cent. A few alloys, which were used in preliminary measurements, were prepared from materials having a purity of 99.9 per cent. Differences between the data obtained from samples prepared from these two grades will be discussed in subsequent sections. The high purity thallium was obtained from the American Smelting and Refining Company. A spectrographic analysis was furnished with this material. This analysis indicated 1 ppm magnesium, <1 ppm lead, <1 ppm copper, and the following elements were listed as not detected: antimony, manganese, tin, silicon, chromium, nickel, bismuth, aluminum, calcium, indium, cadmium, zinc, and silver. By difference the purity of this thallium was 99.999+ per cent. High purity indium was obtained from the Consolidated Mining and Smelting Company of Canada. The purity of this indium was specified as 99.999 per cent, and a typical analysis by the supplier of this grade of indium shows the presence of 2 ppm each of lead and tin and 1 ppm each of copper, thallium,

and cadmium.

All of the alloys used in this investigation were prepared by casting the desired quantities of thallium and indium in Pyrex crucibles which had been coated with Aquadag to facilitate the removal of the alloys. To avoid oxidation the crucibles were either evacuated or filled with helium. The contents of the crucibles were melted with a Meeker burner, homogenized by agitating the molten alloy for a few minutes, and then quenched. In order to minimize composition gradients in the alloys the slugs produced in this manner were formed into rods about 1 mm square and 1 meter long by means of a rod roller, cut into several hundred sections, and recast in the same manner as the original slugs. The electrical resistivity and Debye-Scherrer x-ray data were obtained from wire samples produced by swaging the recast slugs. Sections of some of these wires were rolled to thin foils for use in a symmetrical focusing back reflection powder camera.

Samples for chemical analyses were cut from both ends and the center of several wires in order to check their homogeneity and composition. The two end sections and the center section of each wire were analysed separately for

both indium and thallium. The analytical results on these samples indicated random deviations from the nominal compositions of 0.1 weight per cent along the wires. However, the average of the compositions found for the three sections of any given wire were within 0.02 weight per cent of the nominal composition.

X-ray Measurements

The majority of the diffraction patterns were obtained with a symmetrical back-reflection focusing camera. All of the patterns of the hexagonal phase were obtained with this camera. Some of the patterns of the other phases were obtained with a Debye-Scherrer camera. The samples which were used for the x-ray measurements were annealed for about one hour at a temperature 20-30°C below their respective solidus temperatures. The phase transformations near room temperature are sluggish, therefore, after the samples were annealed they were equilibrated at room temperature for several weeks before being used for the x-ray measurements.

Precision lattice constants of the cubic phases were determined by extrapolating the lattice constant calculated from each reflection against the Nelson-Riley (17) function.

Precision lattice constants for the tetragonal and hexagonal phases were determined by Cohen's method (18). The standard errors calculated for the lattice constants were generally about 0.00005 Å; however, the significance of this number is questionable since the x-ray patterns did not contain a statistically large number of reflections. A more significant measure of the precision of the lattice constants was obtained by comparing the lattice constants calculated from several patterns of the same alloy. These lattice constants generally agreed to within 0.0005 Å. The lattice constants reported in subsequent sections are average values of the lattice constants obtained from several patterns of each alloy.

Determination of Electrical Resistivity

Measurements of relative resistivity values were made on wire samples approximately one millimeter in diameter and one meter long. The resistance was measured by passing a constant current through the sample and measuring the potential difference between two probes with a Leeds and Northrup model K2 potentiometer. At ambient pressure resistivity measurements were made on samples which were wound on a

glass form and submerged in Dow Corning 550 silicone oil. The temperature of the oil was controlled by electrical resistance heating and measured with a calibrated mercury thermometer. Thermal gradients were minimized by continually stirring the oil. The solid-solid phase boundaries were determined from the temperatures at which changes in slopes and/or discontinuities occurred in plots of resistivity versus temperature. At the solidus temperature partial melting of the sample occurred which produced an open circuit. Thence, the solidus temperature was assumed to be the temperature at which the resistance of the sample became infinite.

The samples which were used for resistivity measurements as a function of both pressure and temperature were wound on a teflon form as illustrated in Figure 3. This assembly was placed in a beryllium-copper pressure cell which is shown in Figure 4. The working volume within this cell is a cylindrical region approximately two centimeters in diameter and seven centimeters long. One end of the sample was grounded to the pressure cell by means of a copper strip attached to one end of the teflon holder. The other end was attached to a copper lead which was brought

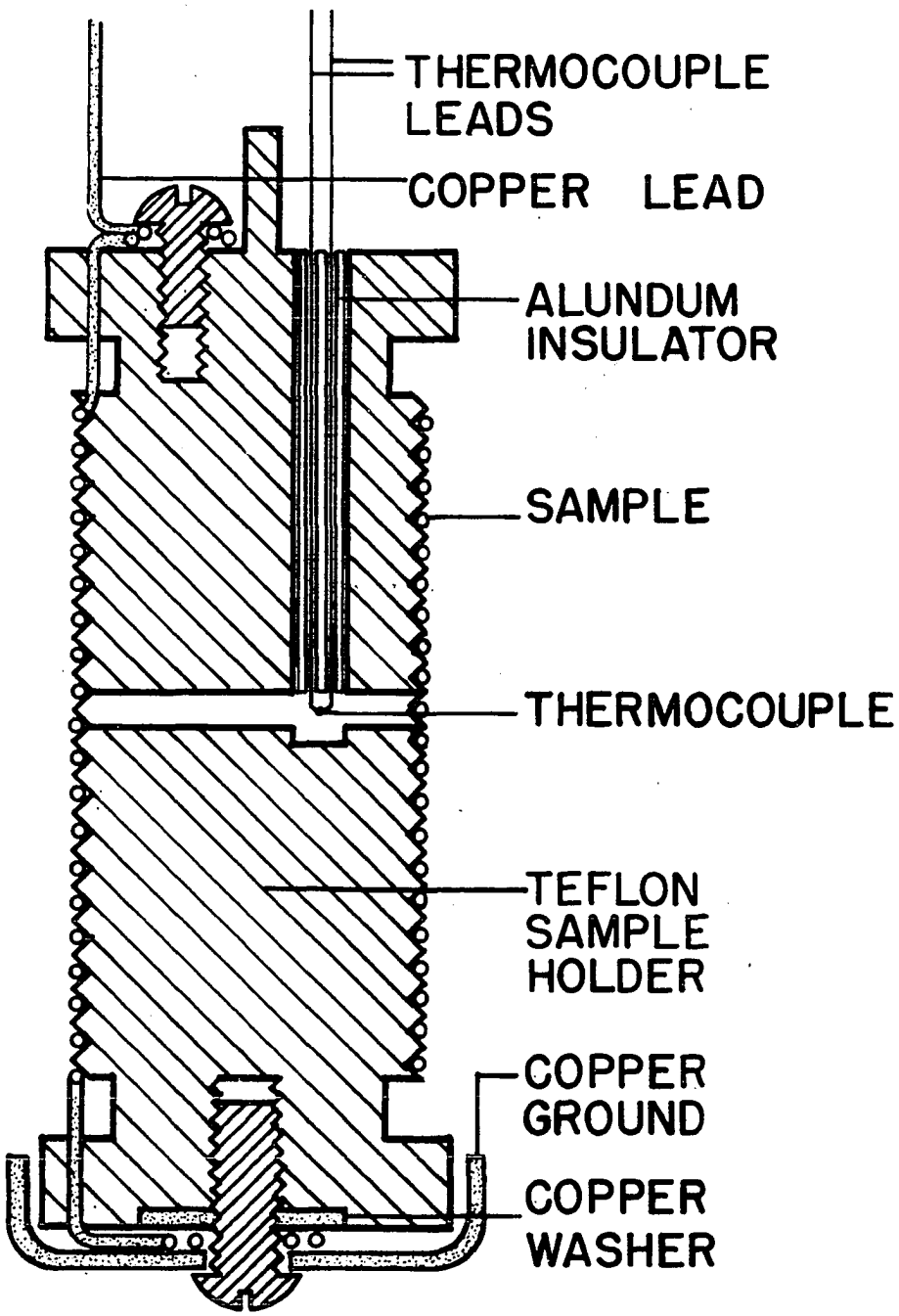

Figure 3. Teflon sample holder

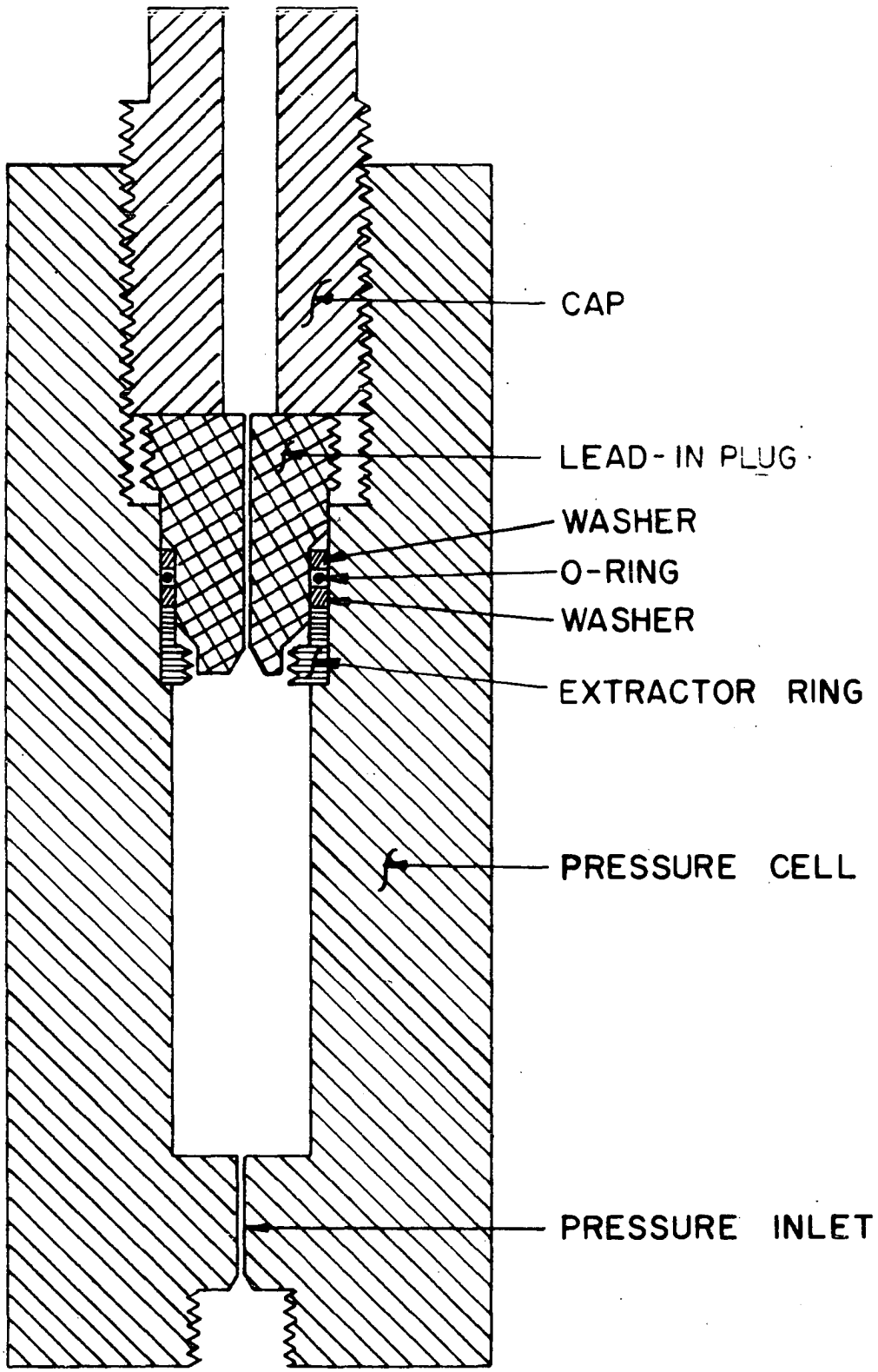

Figure 4. Beryllium-copper pressure cell

into the cell through the lead-in plug. The temperature within the pressure cell was measured with a thermocouple which also entered the cell through the lead-in plug. The temperature of the sample was controlled by submerging the pressure cell in a silicone oil bath similar to the bath described above. Pressure was supplied by means of an intensifier purchased from the Harwood Engineering Company. The pressure fluid was a 1:1 mixture of 10 weight motor oil and white gasoline. A calibrated manganin pressure gauge, also purchased from Harwood, was used to measure the pressure. The calibration of the manganin gauge was checked against a 0-40,000 psi Heise gauge. The precision of the pressure determinations was approximately 10 bars.

At the solidus temperature partial melting of the samples occurs. In order to maintain the sample geometry so that the same sample could be used to determine the solidus temperature at several different pressures the sample holder was modified. The teflon coil form shown in Figure 3 was placed inside a teflon sleeve and the space between the sample, teflon coil form, and teflon sleeve was filled with Wards Bio-Plastic. With this arrangement it was possible to heat the sample above the solidus temperature

and still maintain the sample geometry well enough to determine the solidus temperature by means of the large increase in resistance associated with the onset of the solid to liquid transformation.

RESULTS

X-ray Measurements

The measured lattice constants and c/a ratios of alloys in the face centered tetragonal (FCT) indium phase are shown respectively in Figures 5 and 6 together with values found by Guttman (7) and by Raynor and Graham (19). The results of this investigation agree with the latter two investigations in that a discontinuous transition between the FCT and FCC phases was observed. This statement is based on the fact that a plot of c/a versus composition for the FCT-phase shows that this ratio exceeds unity at the terminus of the FCT-phase. The position of this terminus was established by resistance measurements and its position is in agreement with the results of previous investigations (7,19,20).

The lattice constants of the FCC intermediate phase for alloys in both the FCC region and in the FCC+BCC two-phase region are shown in Figure 7 along with the lattice constants reported by Guttman. The results of this investigation give 59.9 atomic per cent thallium as the position of the FCC/FCC+BCC phase boundary at ambient temperature. This agrees very well with the value of 59.2 atomic per cent thallium reported

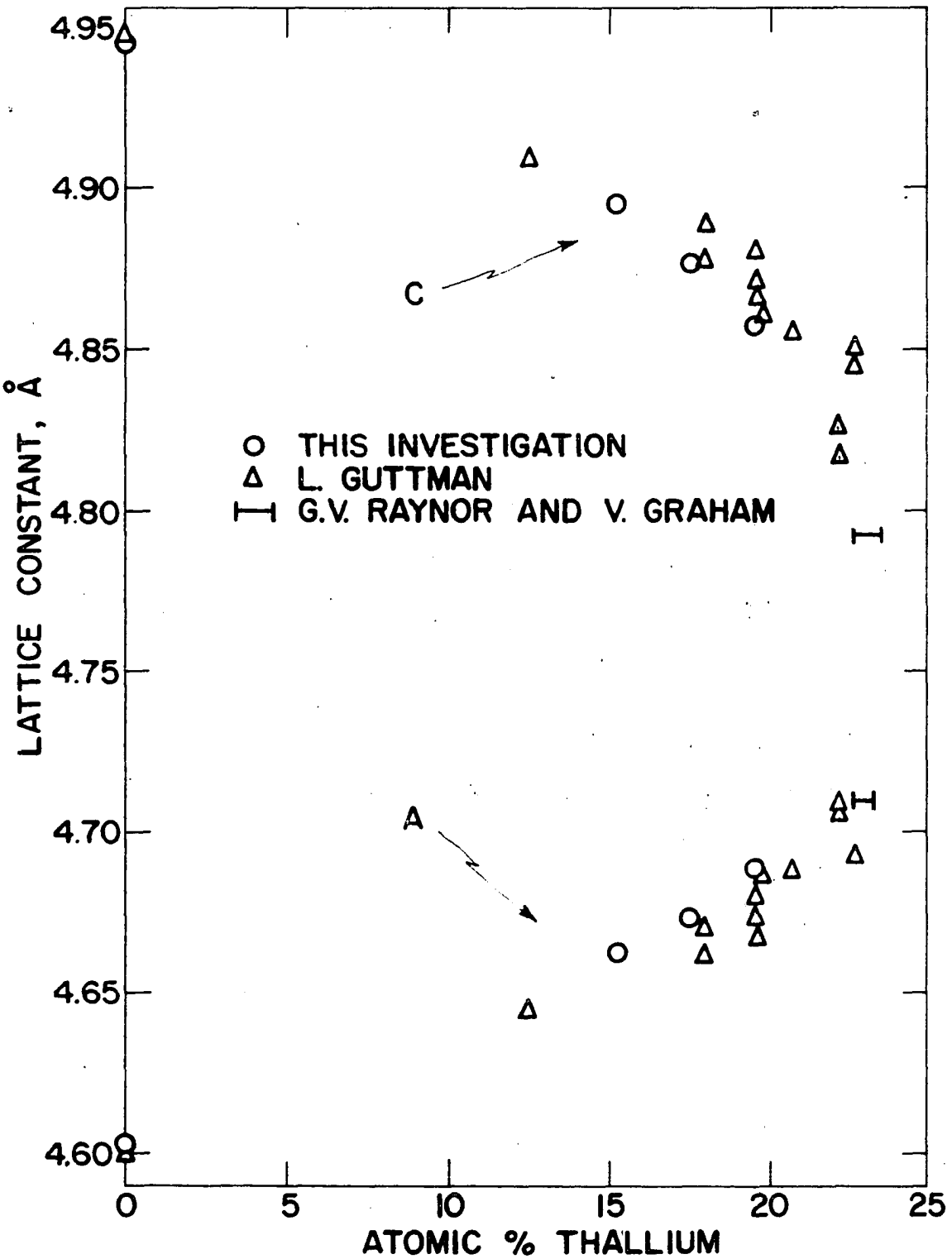

Figure 5. Lattice constants of FCT-indium versus thallium concentration

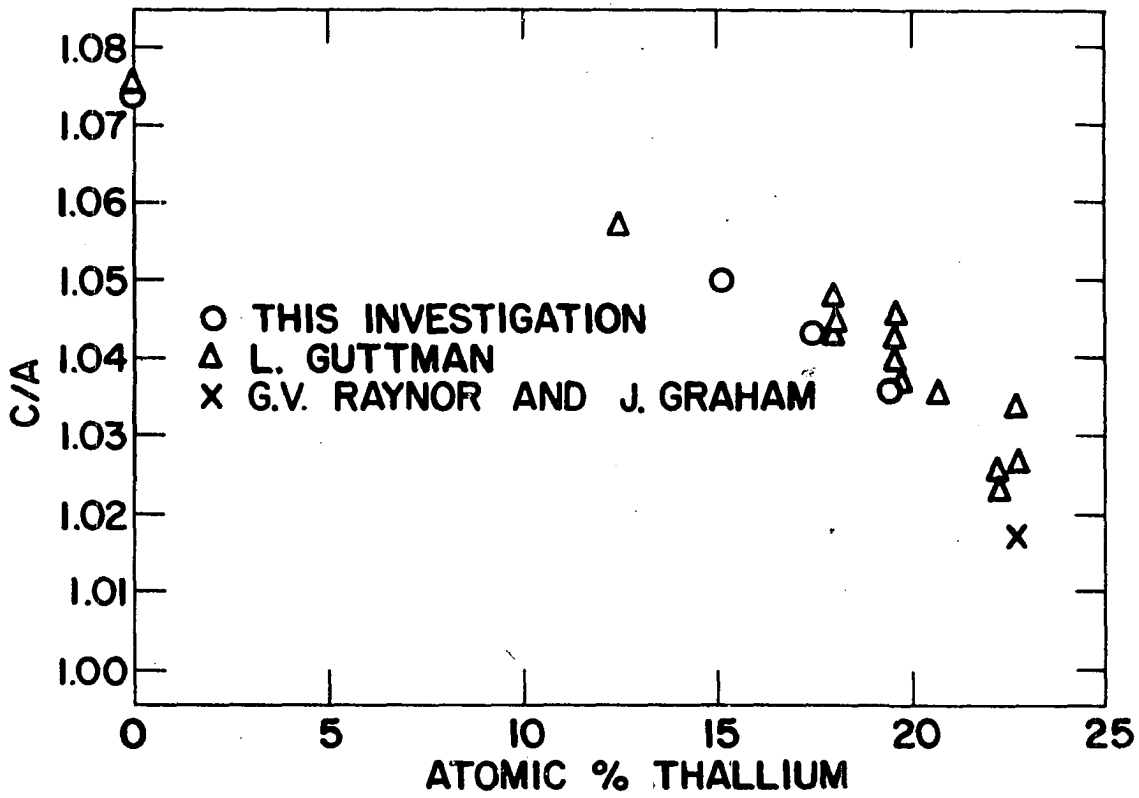

Figure 6. c/a ratio of FCT-indium versus thallium concentration

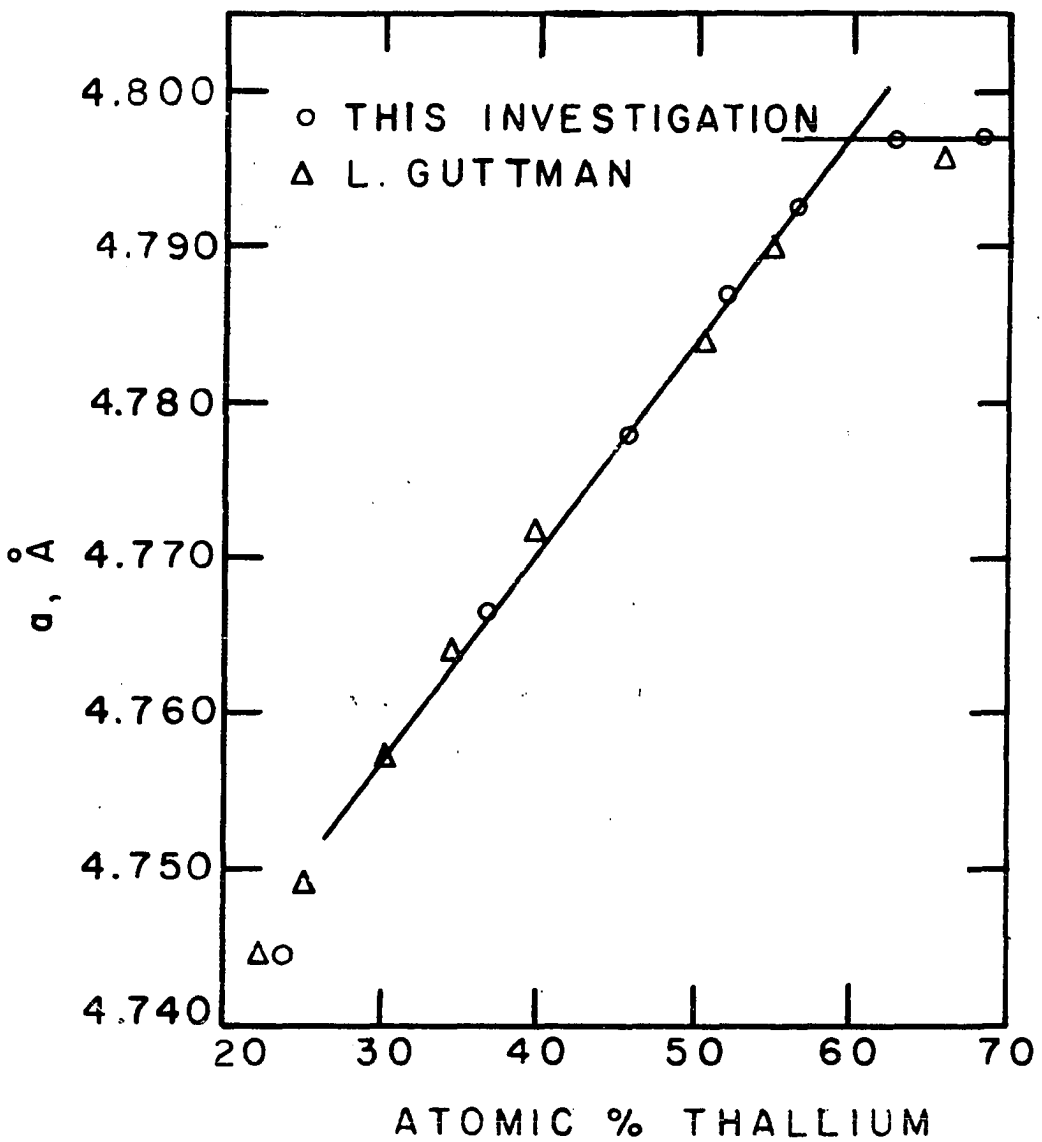

Figure 7. Lattice constant of the intermediate FCC-phase versus thallium concentration

by Guttman.

The values of a, c, and c/a found at room temperatures for pure HCP-thallium were respectively 3.4573 Å, 5.5266 Å, and 1.5985. For these three quantities Lipson and Stokes (21) obtained 3.4566 Å, 5.5248 Å, and 1.5984. Values of the a lattice constant and the c/a ratio of HCP-thallium are shown as a function of indium concentration in Figures 8 and 9. The c lattice constant of HCP-thallium was found to be relatively insensitive to indium concentration. Addition of 11.36 atomic per cent indium decreases this lattice constant by only 0.0008 Å. Thus as indium is added to thallium, both the decrease in volume and the increase in the c/a ratio of the HCP-thallium unit cell are due almost entirely to the decrease of the a lattice constant.

Sekito (16) has reported the existence of a metastable FCC allotrope of thallium at room temperature. Sekito observed this structure in unalloyed thallium which had been quenched from the melt by pouring into ice water. In the present investigation several attempts were made to obtain a FCC allotrope at room temperature. X-ray patterns taken of thallium which had been quenched in the manner described by Sekito did not indicate the presence of a FCC phase. It

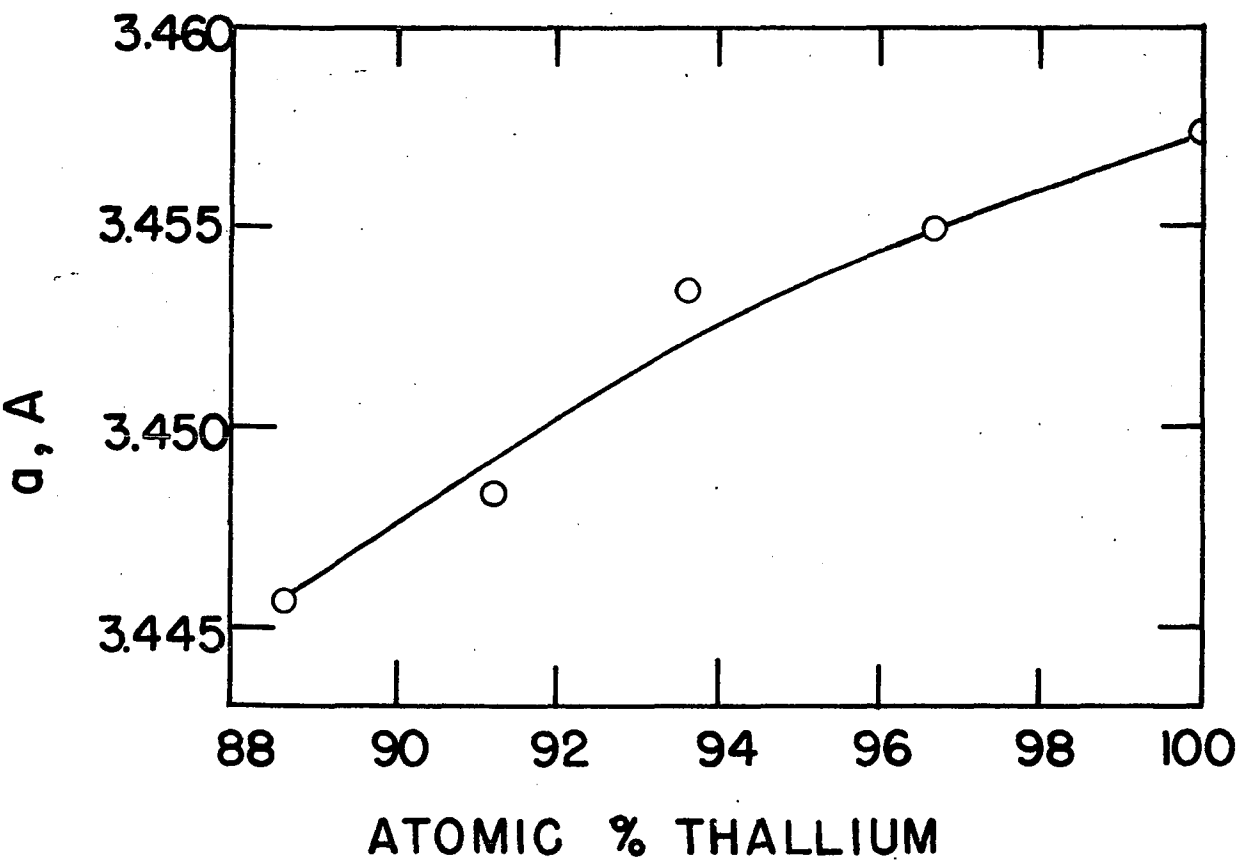

Figure 8. a lattice constant of HCP-thallium alloys versus thallium concentration

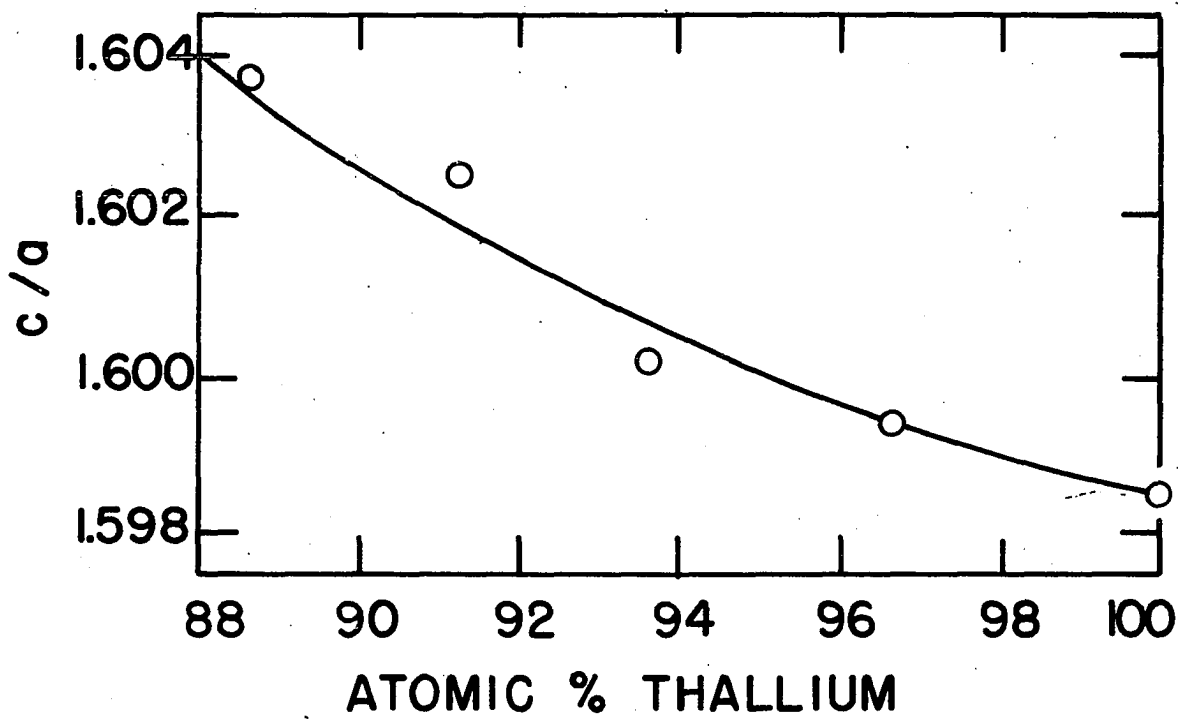

Figure 9. c/a ratio of HCP-thallium alloys versus thallium concentration

is possible that this allotrope can not be obtained at room temperature for high purity thallium and that the thallium used by Sekito contained some impurity which enabled him to obtain a metastable FCC allotrope at room temperature.

Values of the volume per atom as a function of composition calculated from the lattice constants determined in this investigation are plotted in Figure 10. Also shown in this figure are values calculated from the lattice constants reported by Guttman (7) for the indium-rich region of the phase diagram. The solid line shown in Figure 10 represents the volume per atom that would be expected if ΔV of mixing were zero. As may be seen from Figure 10, both the results of Guttman and the present investigation indicate that ΔV of mixing is very small. Bridgman (3) has determined densities of 15 thallium-indium alloys and while these data are inadequate to yield precise values of ΔV of mixing, nonetheless they do give an upper limit for ΔV of mixing comparable to the value indicated in Figure 10. Thus thallium-indium solid solutions are very nearly ideal with respect to volume.

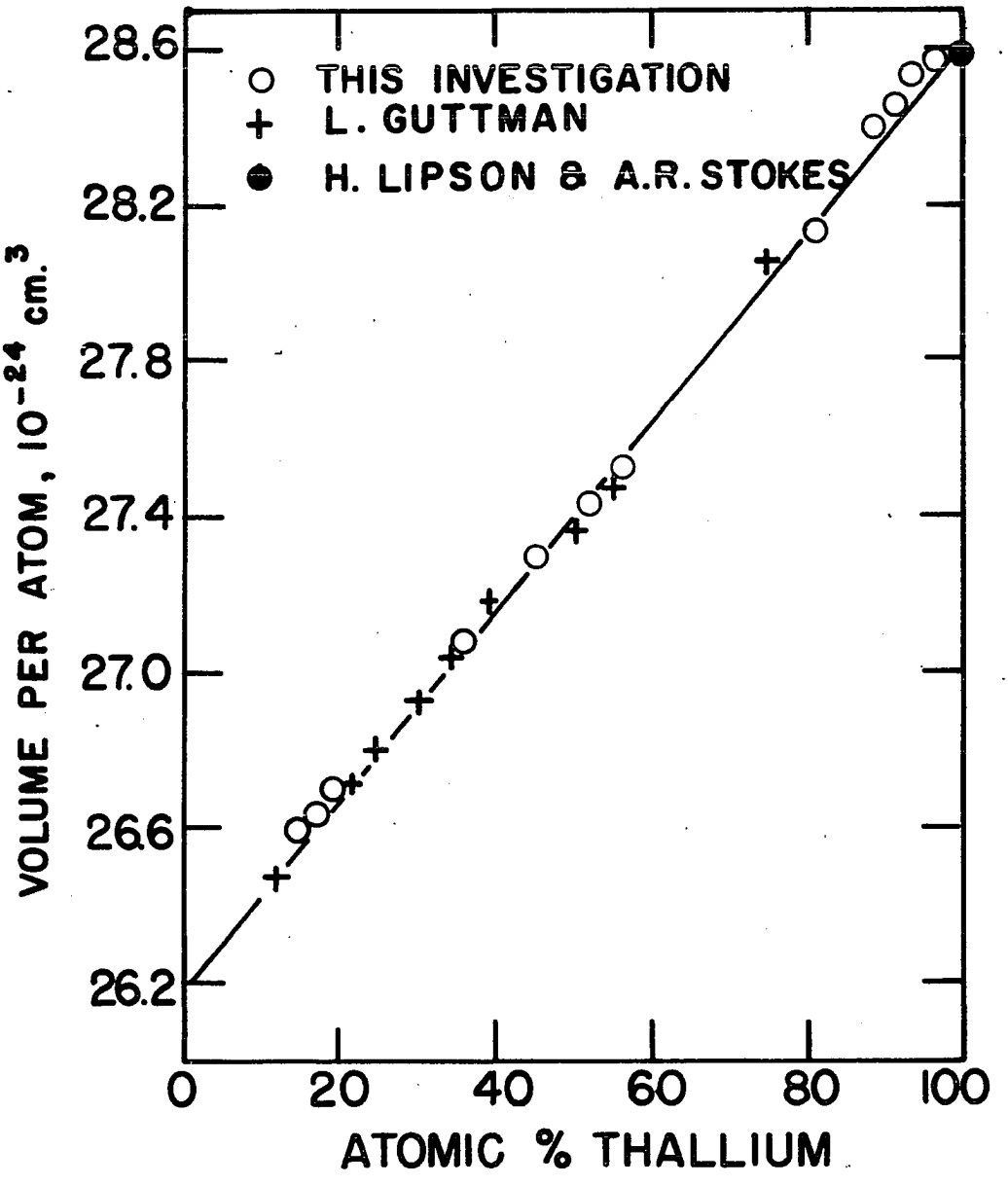

Figure 10. Volume per atom versus thallium concentration

The Thallium-Indium Phase Diagram at Ambient Pressure

The thallium-indium phase diagram based on the results of the present investigation at ambient pressure is shown in Figure 11. Also shown in this figure are the results of Valentiner (8), Guttman (7), and Moore *et al.* (20). The phase diagram shown in Figure 11 differs from the diagram given by Hansen (14), which is shown in Figure 1, in the following respects. The position of the thallium-rich terminus of the peritectic horizontal was found to be at 46 atomic per cent indium compared to a value of about 43 atomic per cent indium on the earlier phase diagram. The results of the present investigation show that the HCP+BCC two-phase region is less than one atomic per cent wide at the eutectoid horizontal and that the eutectoid point is at about 18 atomic per cent indium. The diagram shown in Figure 1, which was based on a limited amount of data, shows the width of the HCP+BCC two-phase region to be about ten atomic per cent with the eutectoid composition being about 24 atomic per cent indium. The experimental evidence supporting a revised diagram with a very narrow HCP+BCC two-phase field is discussed in more detail below.

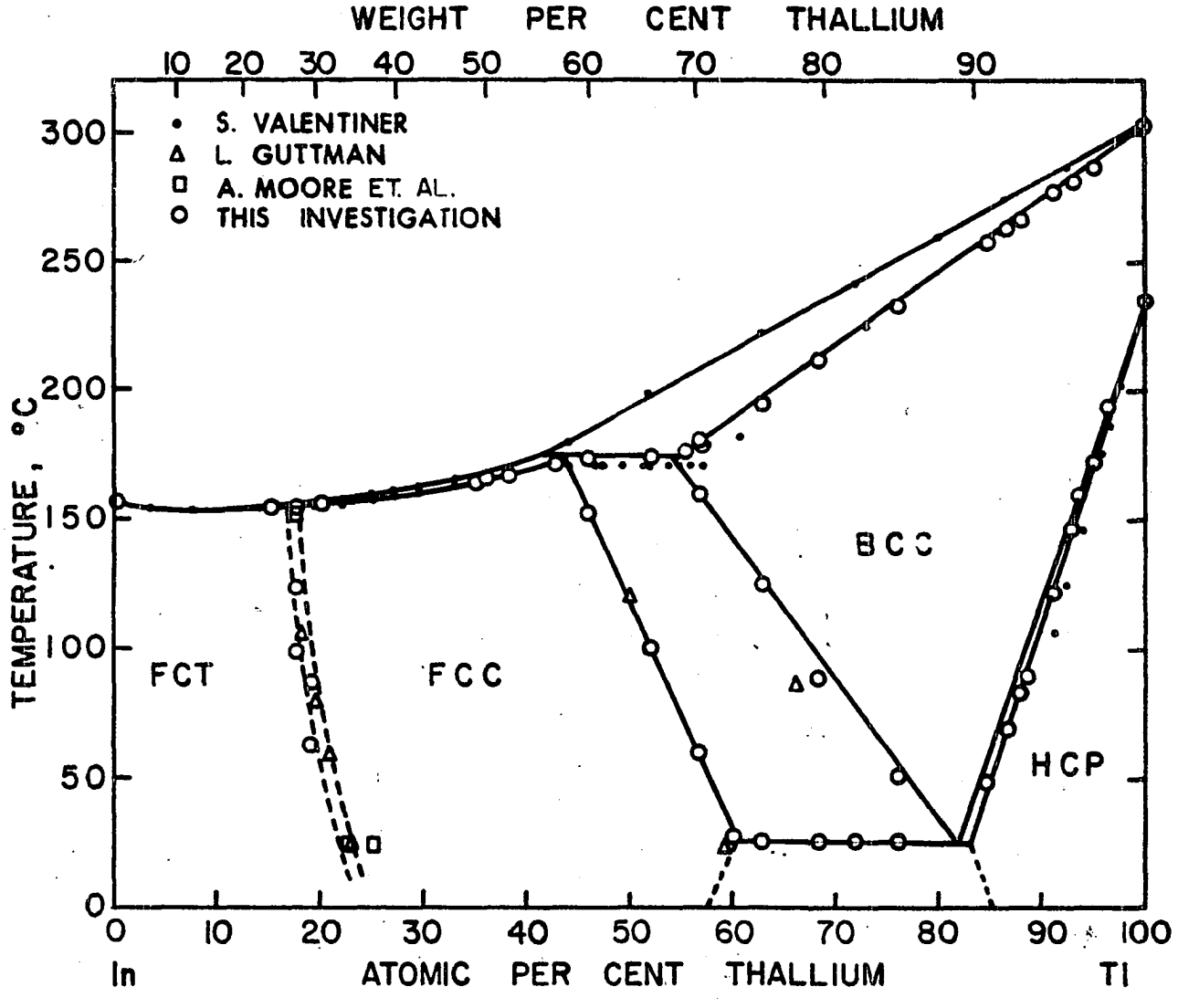

Figure 11. Proposed thallium-indium phase diagram at ambient pressure

Within the precision of the present measurements the change in resistivity accompanying the HCP-BCC transformation of pure thallium occurred isothermally; this is consistent with the phase rule. In the case of thallium containing indium in solid solution the phase rule predicts that the HCP-BCC transformation should occur over a temperature interval rather than isothermally. A typical variation of resistivity of a thallium-indium alloy in the region of the HCP-BCC transformation is shown in Figure 12. The position of the maximum and minimum values of resistivity, on the curve shown in Figure 12, should correspond, respectively, to the onset and conclusion of the HCP-BCC transformation. For all of the alloys these maximum and minimum values were separated by only a few degrees centigrade; this indicates a narrow two-phase field. The intercept of the FCC+BCC/BCC phase boundary on the eutectoid horizontal indicates that the eutectoid composition is very close to the thallium-rich terminus of the eutectoid horizontal; this also supports the conclusion that the HCP+BCC two-phase field is very narrow.

Although the experimental data indicate a narrow two-phase field there is a factor to consider which could affect the validity of this result. This is the possibility that

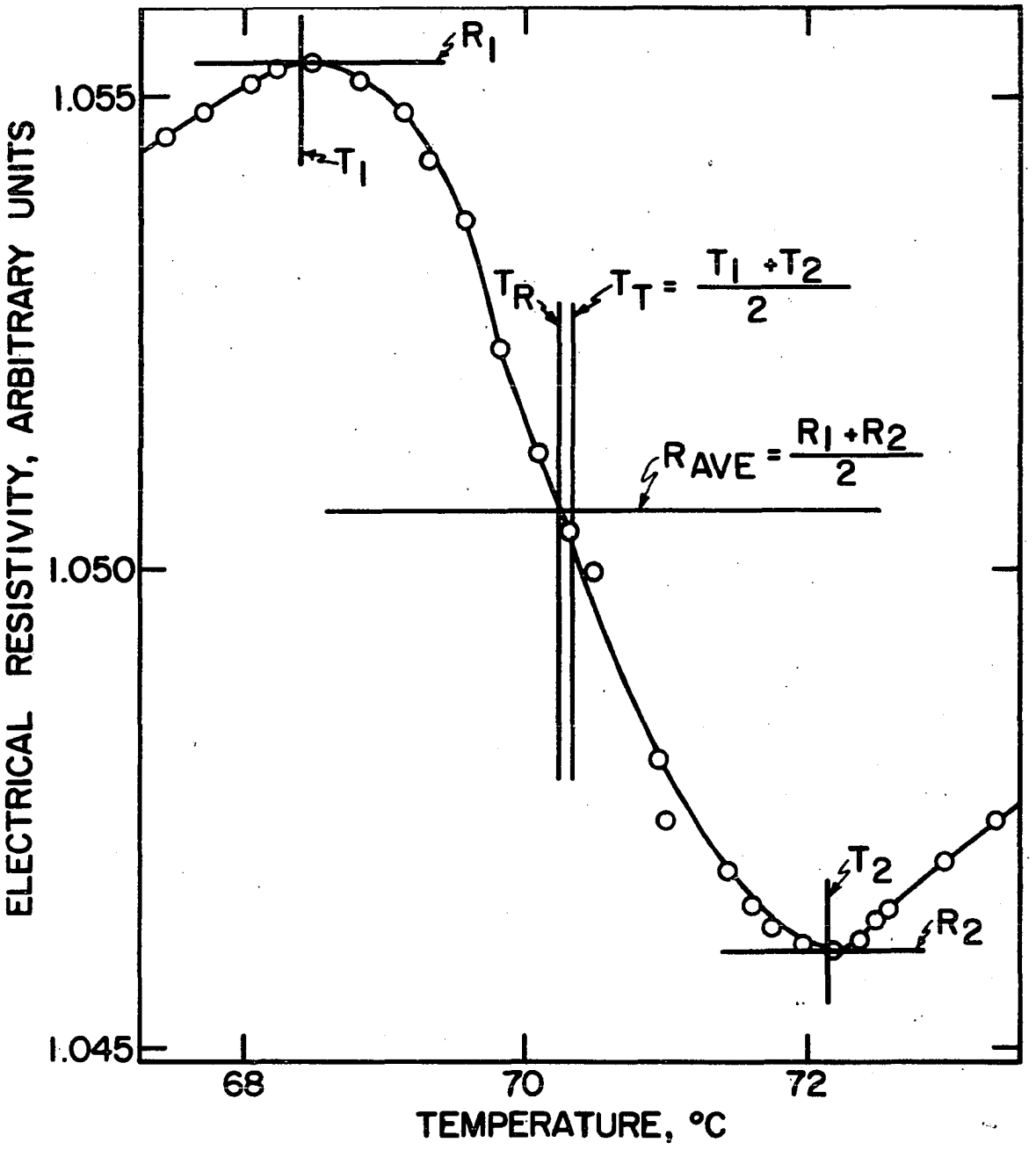

Figure 12. Typical variation of resistivity of a thallium-indium alloy in the region of the HCP-BCC transformation

the observed HCP-BCC transformations occurred under non-equilibrium conditions and that the two-phase region is wider than indicated by the experimental data. Such non-equilibrium conditions would obtain if the HCP-BCC transformation occurred isothermally via a martensitic transformation. Then the temperature interval in which the transformation was observed to occur would be due solely to composition variations in the resistivity samples and not to the presence of a two-phase field. In essence this means that the two-phase region predicted by the phase rule would be quite narrow due to the martensitic nature of the transformation if the time at transformation temperature was inadequate to allow equilibration by diffusion of the atomic species. Some of the evidence indicating that this might be the case is discussed below.

First, composition variations of the magnitude indicated by chemical analyses could account for the temperature intervals in which these transformations were observed to occur. Second, the separations of the boundaries of the two-phase region would normally be expected to increase monotonically with increasing indium addition. The experimental data indicate that this separation varies in a random fashion

with composition; this would indicate that the temperatures at which the onset and conclusion of this transformation were observed did not correspond to the positions of the boundaries of a two-phase region.

Because of the considerations advanced above, mean values of the transformation temperature have been used. T_T and T_R represent two ways of defining a mean transformation temperature from data of the type shown in Figure 12. T_T represents the temperature midway between the temperatures at which the transformation was observed to start and end. T_R represents the temperature at which the resistivity is midway between the values observed at the start and end of the transformation. T_T and T_R, which generally agreed to within a few tenths of a degree, were averaged to obtain the mean transformation temperature.

Values of this mean transformation temperature ($T_{HCP-BCC}$) at ambient pressure are given in Table 1. The results of several sets of measurements on 99.9 and 99.999 per cent thallium indicate that the temperature at which the HCP-BCC transformation occurs for the 99.999 per cent thallium is $2^{o}C$ higher than the temperature at which this transformation occurs for the lower purity thallium. No

significant difference was observed, however, between the transformation temperatures found on alloys which were prepared from these two grades of thallium. The data given in Table 1 indicate that the mean transformation temperature at ambient pressure can be approximated by Equation 1,

$$T_{HCP-BCC} = 234 - 1.2 \times 10^3 N_2 , \qquad (1)$$

where $T_{HCP-BCC}$ is in ^oC and N_2 is the mole fraction of indium.

The Effect of Pressure on the Thallium-Indium Phase Diagram

The effect of pressure on the temperature of the HCP-BCC transformation was determined from resistivity measurements on alloys containing 3.32, 6.37, 8.74, and 11.36 atomic per cent indium. The observed mean transformation temperatures ($T_{HCP-BCC}$) for these alloys at various pressures are tabulated in Table 2. Within the precision of these data the variation of $T_{HCP-BCC}$ with pressure was linear. Values of $T_{HCP-BCC}$ representing linear least squares fits to the experimental data are also included in Table 2. Values of $dT_{HCP-BCC}/dP$ for these four alloys, which were also obtained from these least squares fits, are given in Table 3. A

linear representation of the variation of $dT_{HCP-BCC}/dP$ with composition is

$$\frac{dT_{HCP-BCC}}{dP} = -(2.03 \pm 0.04) - (17.1 \pm 0.5)N_2 \ , \qquad (2)$$

where $T_{HCP-BCC}$ is in ^{o}C, P in kbars, and N_2 is the mole fraction of indium. The validity of this linear representation can be inferred from a comparison in Table 3 of values from Equation 2 with the experimentally determined values. The intercept of Equation 2 lies between the values for pure thallium of -1.96 ^{o}C/kbar found by Bridgman (10) and -2.11 ^{o}C/kbar found by Werner (9); thus measurements on alloys extrapolate to a value for pure thallium which is consistent with independently determined values. Integration of Equation 2, using Equation 1 to evaluate the constant of integration, gives Equation 3 which can be used to approximate the mean temperature of the HCP-BCC transformation as a function of both composition and pressure,

$$T_{HCP-BCC} = 234 - 1.2 \times 10^3 N_2 - (2.03 + 17.1 N_2)P. \qquad (3)$$

The effect of pressure on the eutectoid temperature (T_E) was determined from measurements made on an alloy containing 28.16 atomic per cent indium. The experimental values of the eutectoid temperature at various pressures are tabulated

in Table 4. A linear representation of these data is

$$T_E = 30 + 3.69\ P \qquad (4)$$

where T_E is in ^{o}C, and P is in kbars. Values from the linear representation are compared with the experimental points in Table 4.

The effect of pressure on the solid $\longrightarrow$ liquid + solid phase boundary was determined for alloys containing 43.16, 44.59, 57.24, 61.72, and 64.96 atomic per cent indium. The experimental results for these alloys are given in Table 5. Within the precision of these data an elevation of 4.9 ^{o}C/kbar occurs for both the peritectic horizontal and the adjacent portions of the solidus line. While these data are inadequate to evaluate precise values for the peritectic composition and the composition of the thallium-rich terminus of the peritectic horizontal as functions of pressure, the data do indicate that at a pressure of 40 kbars these compositions are within a few atomic per cent of the ambient pressure values.

Equations 3 and 4 show that as pressure increases the eutectoid temperature increases while the HCP-BCC transformation temperature decreases with a concomitant decrease of the solubility of indium in HCP-thallium. Extrapolation of

this result to higher pressures predicts the existence of a triple point in pure thallium at 162°C and 35.8 kbars. The crystal structures of the phases in equilibrium at this triple point are HCP, BCC, and FCC. The HCP and BCC phases are continuous with the HCP low temperature phase and the BCC high temperature phase which are observed in pure thallium at ambient pressure. The FCC-phase is continuous with the FCC-phase which is stable at ambient pressure from 40 to 77 atomic per cent indium. At pressures several kbars above the triple point the HCP-phase no longer exists and the stable low temperature form of thallium is FCC. Isobaric sections of the proposed thallium-rich portion of the thallium-indium phase diagram are shown in Figure 13 for ambient pressure and for pressures of 5, 30, and 40 kbars. The melting points of pure thallium shown in these isobaric sections are based on the data of Butuzov *et al.* (22). The remaining portion of the isobaric sections for ambient pressure and for 5 kbars were constructed on the basis of the results of the present investigation, while the sections for 30 and 40 kbars are based on extrapolation of the observed pressure dependence.

Figure 13. Isobaric sections of the thallium-rich region of the proposed thallium-indium phase diagram

The sections shown for ambient pressure and 5 kbars are based on experimental results

The sections shown for 30 and 40 kbars were obtained by extrapolation of the observed pressure dependence

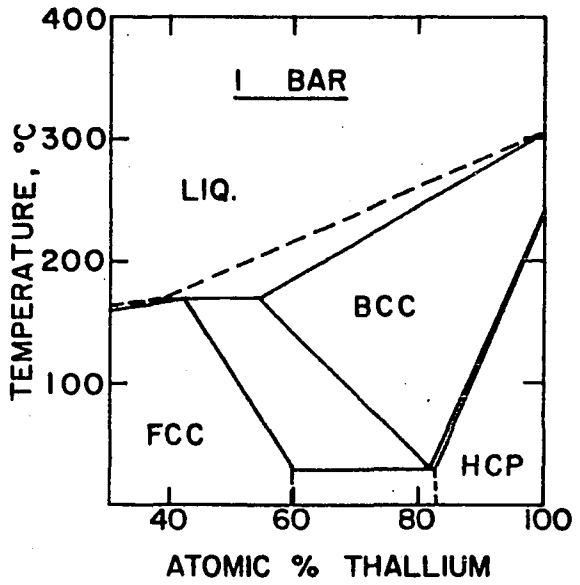
1 BAR
LIQ.
BCC
FCC
HCP
TEMPERATURE, °C
400
300
200
100
40
60
80
100
ATOMIC % THALLIUM

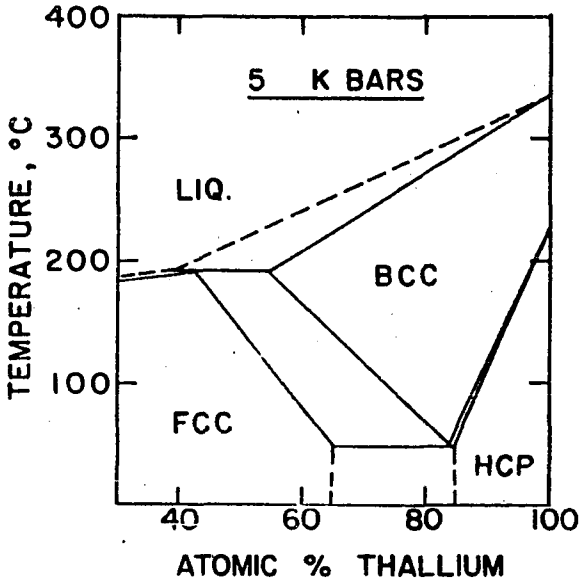
5 K BARS
LIQ.
BCC
FCC
HCP
TEMPERATURE, °C
400
300
200
100
40
60
80
100
ATOMIC % THALLIUM

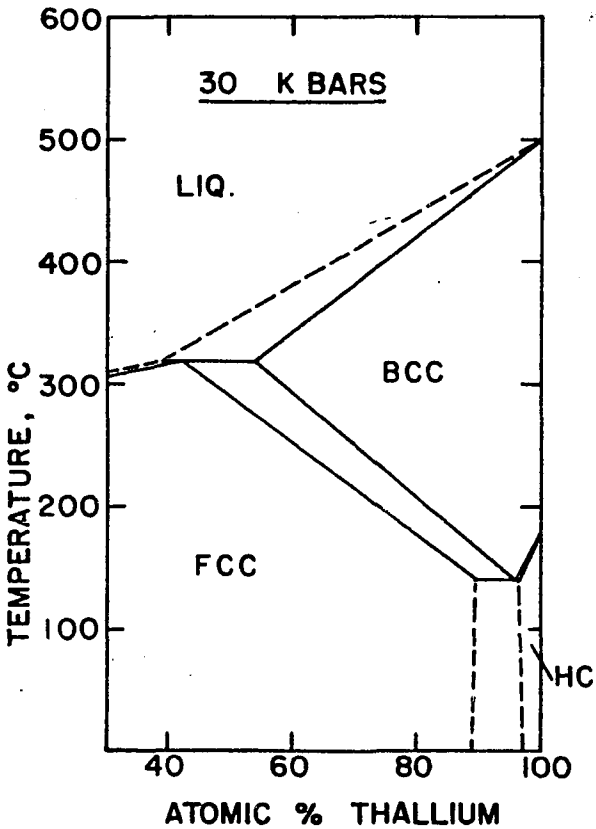
30 K BARS
LIQ.
BCC
FCC
HCP
TEMPERATURE, °C
600
500
400
300
200
100
40
60
80
100
ATOMIC % THALLIUM

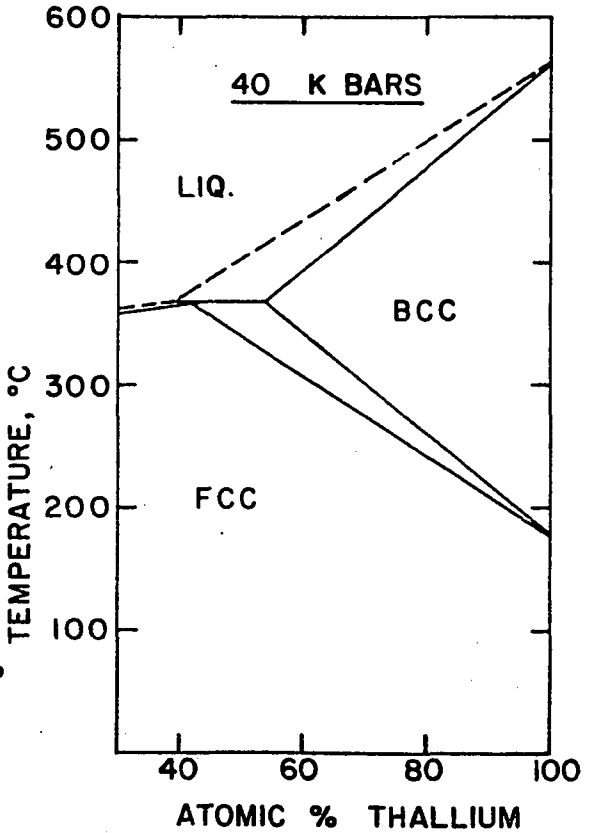
40 K BARS
LIQ.
BCC
FCC
TEMPERATURE, °C
600
500
400
300
200
100
40
60
80
100
ATOMIC % THALLIUM

DISCUSSION

The isobaric sections of the phase diagram in Figure 13 show that the crystal structure of the high pressure allotrope of thallium is face centered cubic. While this conclusion is based on an extrapolation over a relatively large range of pressure there is a considerable amount of evidence justifying both the extrapolation and the conclusion as to the crystal structure.

First, on the basis of a thermodynamic calculation Kaufman (23) has suggested that the crystal structure of the high pressure allotrope of thallium is FCC. Although Kaufman's calculation is based on approximations, his conclusion is in agreement with the results of the present investigation.

Second, a comparison of Bridgman's (3) results with the room-temperature isothermal section of the thallium-rich region of the proposed thallium-indium phase diagram is shown in Figure 14. Bridgman notes in his paper that he observed the transformations to occur over a range of pressure as would be expected on the basis of the phase rule; however, his tabulated data are smoothed and indicate only

Figure 14. Room temperature isothermal section of the thallium-rich region of the proposed thallium-indium phase diagram

O - Transformation pressure determined from pressure-volume measurements made with increasing pressure

X - Transformation pressure determined from resistivity measurements made with increasing pressure

Δ - Transformation pressure determined from pressure-volume measurements made with decreasing pressure

+ - Transformation pressure determined from resistivity measurements made with decreasing pressure

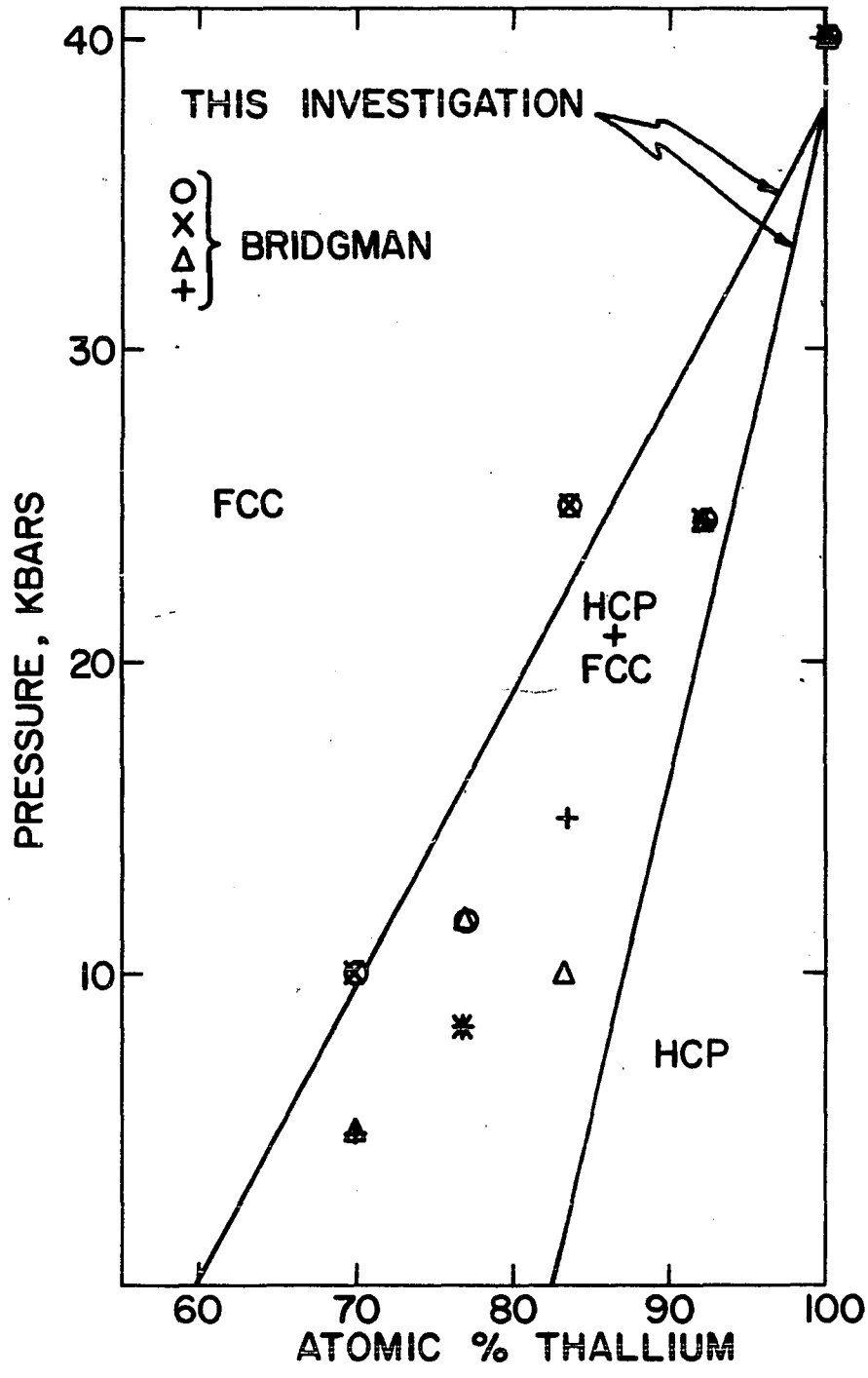
THIS INVESTIGATION
BRIDGMAN
FCC
HCP
+
FCC
HCP
PRESSURE, KBARS
ATOMIC % THALLIUM
40
30
20
10
60
70
80
90
100

a single point for each observed transformation. On this basis it is impossible to make a quantitative comparison of his experimental observations with the results of the present investigation. Qualitatively, however, the agreement between Bridgman's results and the diagram herein proposed is quite adequate.

Finally, extrapolation of the pressure dependence of the phase transformations observed in this investigation indicates that the triple point in pure thallium should occur at 162°C and 35.8 kbars. Bridgman (10) has reported the triple point of pure thallium to be at 153°C and 38.3 kbars. At ambient pressure Bridgman found the HCP-BCC transformation in thallium to occur at 227°C, while the high purity thallium which was used in this investigation was observed to undergo this transformation at 234°C. Further, at ambient temperature Bridgman observed the transformation of the HCP allotrope to a high pressure form at 40.3 kbars, while Boyd and England (12) and Kennedy and LaMori (11) found, respectively, 37.1 and 36.7 kbars. If the slopes in Bridgman's temperature-pressure diagram are correct, extrapolations of the transformation at ambient pressure and 234°C and of the transformation at ambient temperature and a mean pressure of 36.9

kbars indicate the position of the triple point to be at 167°C and 34.7 kbars. Since the triple point as determined in this investigation lies between this latter position and the position reported by Bridgman (10), the extrapolation of the phase fields to high pressures appears to be justified. Thence, the conclusion as to the crystal structure of the high pressure allotrope appears to be valid.

SUMMARY

The results of this investigation show that the crystal structure of the high pressure allotrope of thallium is face centered cubic. Extrapolation of the results of the present investigation shows a triple point at 162°C and 35.8 kbars between the FCC, BCC, and HCP allotropes of thallium.

A revised phase diagram for the thallium-indium system at ambient pressure is proposed. This diagram agrees in general form with the previously reported phase diagram, but there is a marked difference in detail in regard to the eutectoid composition and the width of the HCP+BCC two-phase region. The revised eutectoid composition is within about one atomic per cent of the thallium-rich terminus of the eutectoid horizontal, thus the width of the HCP+BCC two-phase region is quite narrow.

LITERATURE CITED

1. Bridgman, P. W. Proc. Am. Acad. Arts Sci. 82, 101 (1953).

2. Bridgman, P. W. Proc. Am. Acad. Arts Sci. 83, 151 (1954).

3. Bridgman, P. W. Proc. Am. Acad. Arts Sci. 84, 1 (1955).

4. Bridgman, P. W. Proc. Am. Acad. Arts Sci. 84, 43 (1955).

5. Bridgman, P. W. Proc. Am. Acad. Arts Sci. 84, 131 (1957).

6. Bridgman, P. W. Proc. Am. Acad. Arts Sci. 84, 179 (1957).

7. Guttman, L. Trans. Am. Inst. Min., Met., and Pet. Eng. 188, 1472 (1950).

8. Valentiner, S. Z. Metallkunde 32, 244 (1940).

9. Werner, M. Z. anorg. Chem. 83, 275 (1913).

10. Bridgman, P. W. Phys. Rev. 48, (1935).

11. Kennedy, G. C. and LaMori, P. N. Some Fixed Points on the High Pressure Scale. In Bundy, F. P., Hibbard, W. R. and Strong, H. M. eds. Progress in Very High Pressure Research pp 304-313. New York, N.Y., John Wiley and Sons, Inc. 1961.

12. Boyd, F. R. and England J. L. Carnegie Inst. Washington, Year Book 58, 88 (1959).

13. Hansen, M. Der Aufbau der Zweistofflegierungen. Berlin, Julius Springer, 1936.

14. Hansen, M. Constitution of Binary Alloys. 2nd ed. New York, N.Y., McGraw-Hill Book Co., Inc. 1958.

15. Schneider, A. and Heymer, G. Z. anorg. Chem. 286, 118 (1956).

16. Sekito, Sinkiti Z. Krist. 74, 189 (1930).

17. Nelson, J. B. and Riley, D. P. Proc. Phys. Soc. (London) 57, 1960 (1945).

18. Azaroff, L. V. and Buerger, M. J. Powder Method in X-Ray Crystallography. New York, N.Y., McGraw-Hill Book Co., Inc. 1958.

19. Raynor, G. V. and Graham, J. Trans. Faraday Soc. 54, 161 (1958).

20. Moore, A., Graham, J., Williamson, G. K. and Raynor, G. V. Acta. Met. 3, 579 (1955).

21. Lipson, H. and Stokes, A. R. Nature 148, 437 (1941).

22. Butuzov, V. P., Royatovskii, E. G. and Shakhovskoi, G. P. Doklady Akad. Nauk. S.S.S.R. 109, 519 (1954).

23. Kaufman, L. Acta. Met. 9, 896 (1961).

ACKNOWLEDGMENTS

The author wishes to express his appreciation to Dr. J. F. Smith for his interest and assistance throughout this work. The author is also indebted to Dr. R. G. Barnes for the generous loan of the pressure cell used in this investigation, to Dr. C. V. Banks and Mr. M. J. Tschetter for carrying out chemical analyses of several of the alloys used in this investigation, and to Dr. C. A. Swenson for several interesting and informative discussions.

APPENDIX

Table 1. Mean HCP-BCC transformation temperature at ambient pressure

Atomic % indium	Mean temperature, °C
0.00[a]	234
0.00[b]	232
3.32	194
5.21	172
6.37	160
7.18	146
8.74	125
8.95	122
11.36	90
12.27	83
13.44	69
15.47	49

[a]99.999 per cent thallium

[b]99.9 per cent thallium

Table 2. Mean HCP-BCC transformation temperature

Atomic % indium	Pressure, kbars	Mean temperature, °C (observed)	Mean temperature °C (least squares fit)
3.32	1.38	191.1	190.7
3.32	2.55	187.9	187.6
3.32	3.50	185.1	185.2
3.32	0.00	194.2	194.3
3.32	1.98	188.7	189.1
6.37	1.04	157.0	157.0
6.37	3.46	149.6	149.6
6.37	5.53	143.0	143.2
6.37	4.69	145.9	145.7
6.37	2.42	153.0	152.8
6.37	0.00	160.2	160.3
8.74	1.03	122.2	120.9
8.74	3.23	113.7	113.1
8.74	5.53	104.6	104.9
8.74	4.76	107.5	107.7
8.74	2.19	116.7	116.8
8.74	0.00	124.5	124.6
8.74	0.00	124.0	124.6
8.74	0.00	124.1	124.6
11.36	0.89	86.4	86.6
11.36	3.01	77.4	78.1
11.36	2.94	78.3	78.5
11.36	0.00	90.9	90.1
11.36	5.37	69.1	68.8
11.36	5.32	69.3	69.0
11.36	0.00	89.9	90.1

Table 3. Variation of mean HCP-BCC transformation temperature with pressure

Atomic % indium	$dT_{HCP-BCC}/dP$, °C/kbar (observed)	$dT_{HCP-BCC}/dP$ °C/kbar (least squares fit)
0.00	---	2.03
3.32	2.61 ± .14	2.60
6.37	3.09 ± .04	3.12
8.74	3.55 ± .11	3.54
11.36	3.98 ± .09	3.98

Table 4. Eutectoid temperature

Pressure, kbars	Eutectoid temperature, °C (observed)	Eutectoid temperature, °C (least squares fit)
0.82	32.2	33.0
3.18	42.1	41.7
0.00	30.0	29.9
2.09	38.5	37.6
5.67	50.5	50.9
5.65	51.1	50.8
4.57	46.1	46.8
2.54	39.7	39.3
0.00	29.7	29.9

Table 5. Solid → solid + liquid transformation temperature

Atomic % indium	Pressure kbars	$T_{s \rightarrow s+l}$, °C (observed)	$T_{s \rightarrow s+l}$, °C (least squares fit)
43.16	1.08	185.2	185.4
43.16	2.09	190.5	190.8
43.16	3.64	198.8	199.0
43.16	2.71	194.7	194.1
43.16	0.00	179.8	179.7
44.59	0.97	181.5	181.9
44.59	0.93	181.3	181.6
44.59	0.00	177.4	177.3
44.59	2.47	188.3	188.8
44.59	2.44	188.1	188.7
44.59	2.89	191.5	190.8
44.59	3.13	192.3	191.9
44.59	0.00	177.9	177.3
57.24	3.43	189.2	189.2
57.24	1.08	176.4	177.0
57.24	2.24	183.0	183.1
57.24	4.49	194.3	194.6
57.24	5.48	200.2	199.7
57.24	0.00	172.1	171.5
61.72	0.99	177.2	172.0
61.72	2.30	178.2	178.1
61.72	4.05	185.8	186.1
61.72	5.34	192.4	192.1
61.72	4.37	187.6	187.6
61.72	3.15	181.8	182.0
61.72	0.00	167.4	167.5
64.96	0.82	168.2	168.1
64.96	3.08	179.4	178.8
64.96	2.44	175.8	175.8
64.96	3.86	182.2	182.5
64.96	1.71	171.9	172.3
64.96	0.00	164.3	164.3